Electronic Supplementary Material (ESI) for Nanoscale.

A chemisorbed interfacial layer for seeding atomic layer deposition on graphite

Anton Brown,[1‡] John Greenwood,[1,2‡] César J. Lockhart de la Rosa,[3] Miriam C. Rodríguez González,[1] Ken Verguts,[3] Steven Brems,[3] Haodong Zhang,[3] Brandon E. Hirsch,[1] Stefan De Gendt,[3] Annelies Delabie,[3] Matty Caymax,[3] Joan Teyssandier,[1,4] Steven De Feyter*[1]*

[1]Division of Molecular Imaging and Photonics, Department of Chemistry, KU Leuven-University of Leuven, Celestijnenlaan, 200 F, 3001 Leuven, Belgium

[2]Present address: QinetiQ, Advanced Services and Products, A7 Building, Cody Technology Park, Ively Road, Farnborough, Hampshire, GU14 0LX, United Kingdom.

[3]imec, Kapeldreef 75, B-3001 Leuven, Belgium

[4]Present address: Institut de Sciences des Matériaux de Mulhouse, CNRS-UMR 7361, Université de Haute Alsace, 3Bis, rue Alfred Werner, 68093 Mulhouse, France

‡: contributed equally

Corresponding authors: joan.teyssandier@gmail.com, steven.defeyter@kuleuven.be

Formation and characterization of the chemisorbed layer. HOPG was first covalently modified with a dense layer of aryl species using cyclic voltammetry. The electrochemical modification was carried out in an aqueous solution containing diazonium cations generated *in situ* from stable aniline precursors - reaction scheme shown in figure S1a. Incorporating sterically hindering substituents on the aniline precursor limits or prevents the formation of multilayers. After diazotization, the mechanism of covalent attachment involves reduction of the diazonium cation, expulsion of N_2 and formation of aryl radicals. These unstable aryl radicals subsequently react with the graphitic surface, see figure S1b. The result is a newly formed sp^3 hybridized carbon-carbon bond that covalently links the aryl species to the surface carbon lattice.

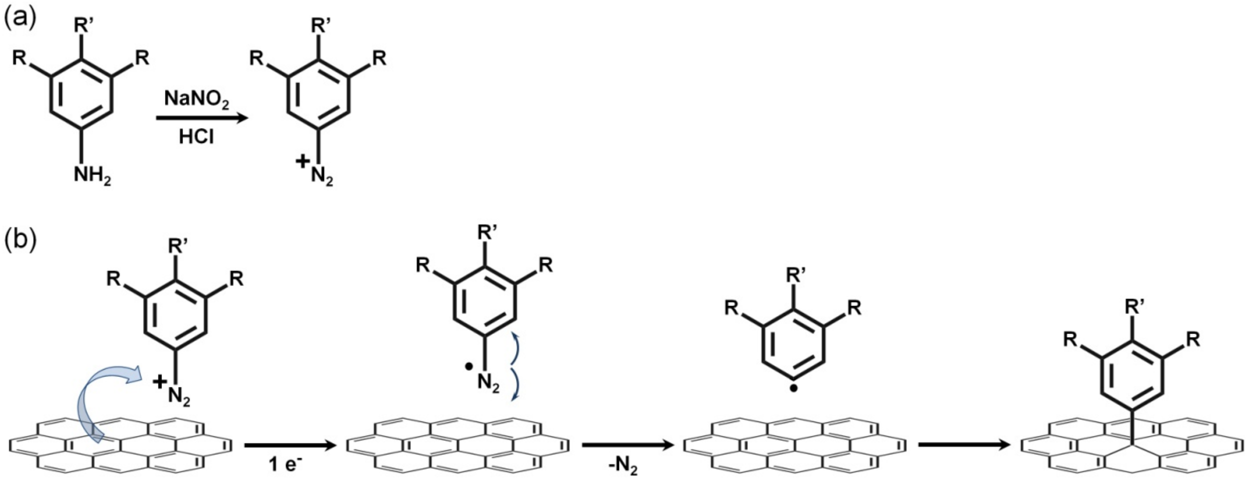

Figure S1. (a) Reaction sequence of conversion of the aniline precursor to the diazonium salt. For TBD: R = *tert*-butyl and R' = H; for TMeOD: R = R' = OMe. (b) Reaction scheme for the generation and covalent attachment of aryl radicals to the carbon surface.

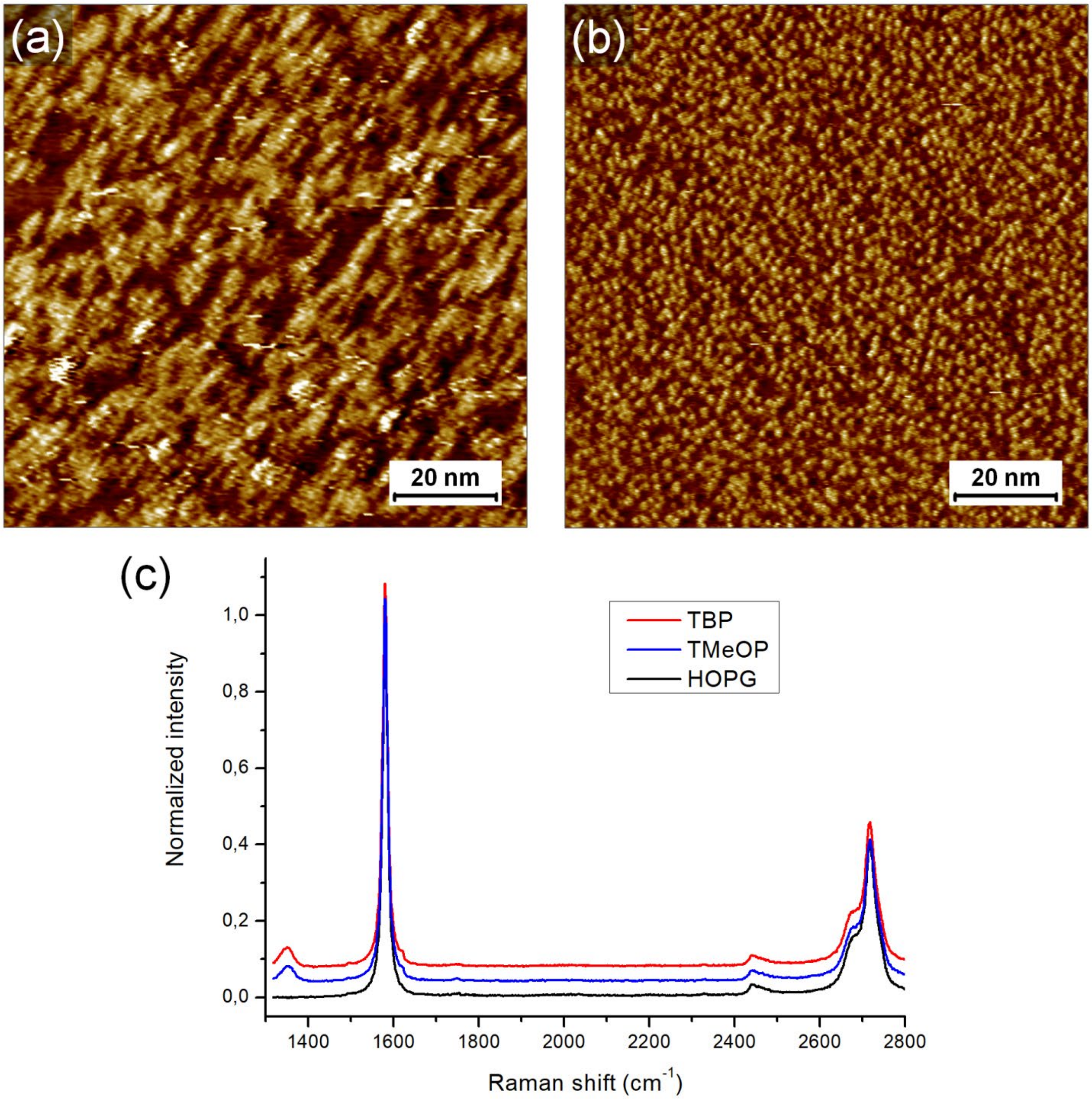

Figure S2. STM images of high density (a) TMeOP and (b) TBP layers on HOPG. (c) Raman spectra of HOPG, TMeOP and TBP samples in the range 1300-2800 cm^{-1}.

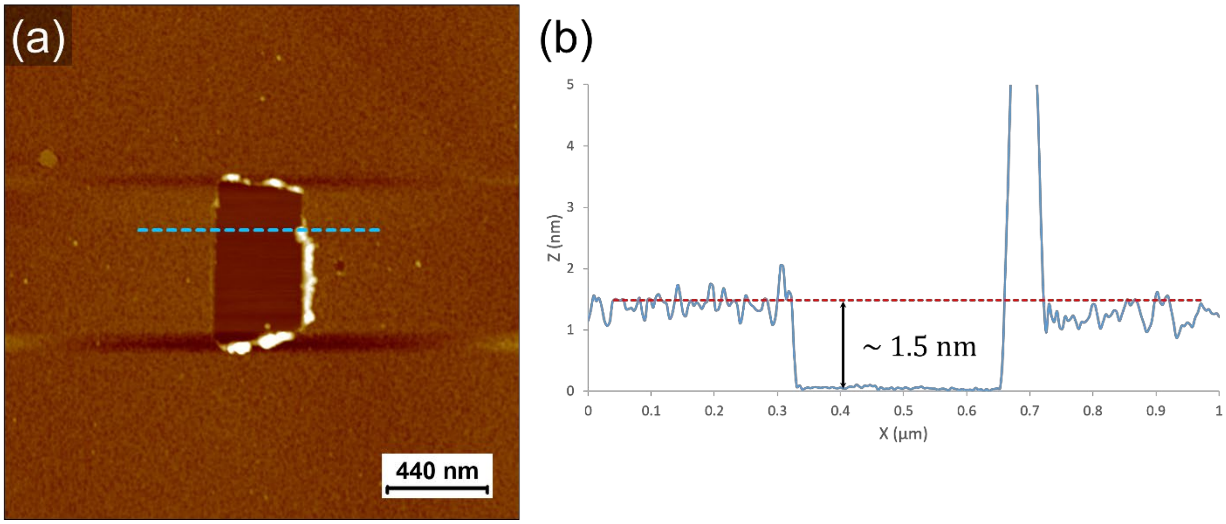

Figure S3. (a) AFM topography image of a TMeOP-functionalized HOPG sample. The darker rectangle in the center corresponds to the area nanoshaved by the AFM tip (i.e. HOPG surface). (b) Line profile along the blue dotted line in (a). Nanoshaving consists in mechanical scratching of the film in a defined square using AFM. In this method, molecules are removed by sweeping them away with the AFM tip, whilst the machine is operated in contact mode (force applied ~ 20 nN). The nanoshaved region is then image in tapping mode, allowing precise determination of the height of the molecular layer. For the nanoshaving experiments (scratching + imaging), AC240TS-R3 cantilevers (Olympus) were used.

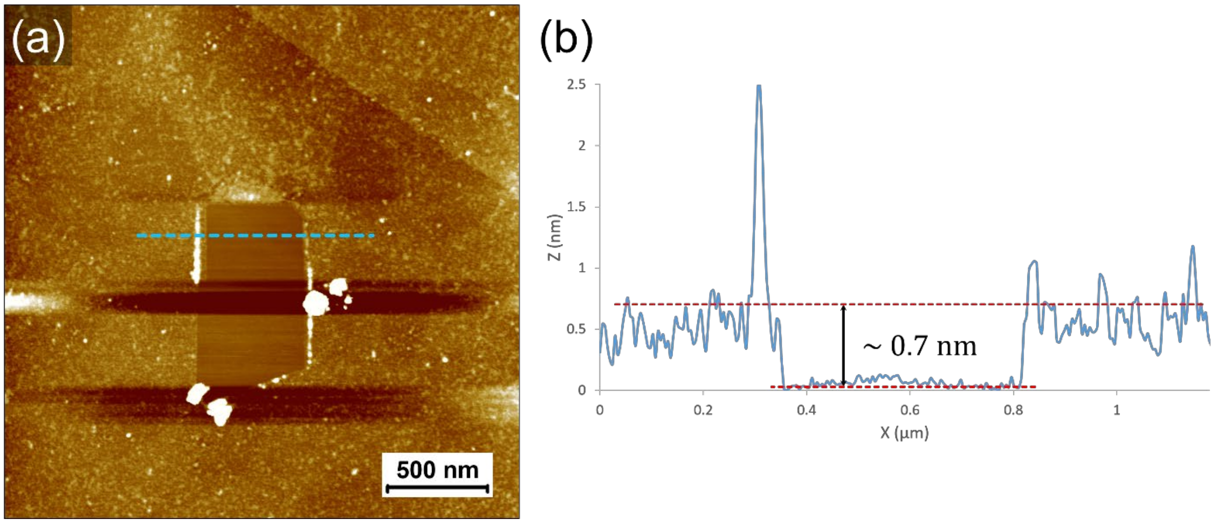

Figure S4. (a) AFM topography image of a TBP-functionalized HOPG sample. The darker rectangle in the center corresponds to the area scratched by the AFM tip (i.e. HOPG surface). (b) Line profile along the blue dotted line in (a). Nanoshaving experiments were performed in the same conditions as for the TMeOP-functionalized sample.

Effects of annealing on covalently modified graphite. Control experiments were performed by subjecting the TBP- and TMeOP-functionalised samples to annealing at 150 °C during a duration equivalent to 80 ALD cycles (80 min). The comparison of AFM images before and after 80 min annealing is shown in figure S5 and S6. For TMeOP, no major changes are observed and the general appearance of the molecular layer is the same. Very little amount of material is leaving the surface, as evidence by the shallow pits in figure S5b. For TBP (figure S6b), more material is gone. Besides, the surface of the top layer appears smoother. The noisy lines in the center part of figure S6b suggest the presence of mobile material.

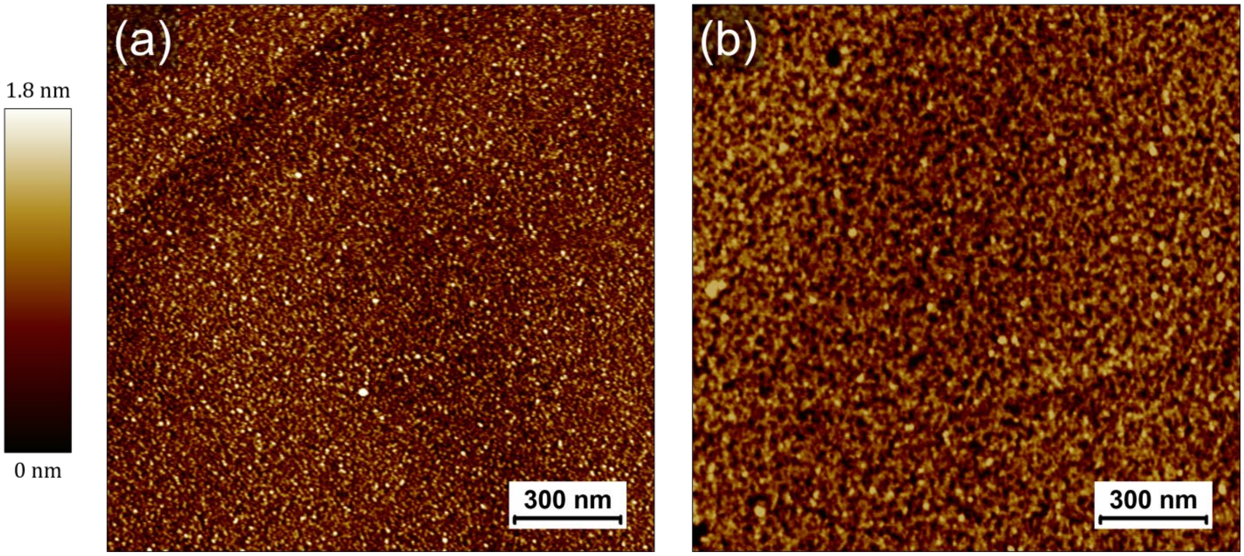

Figure S5. AFM comparison of TMeOP layers on HOPG (a) before and (b) after 80 min annealing.

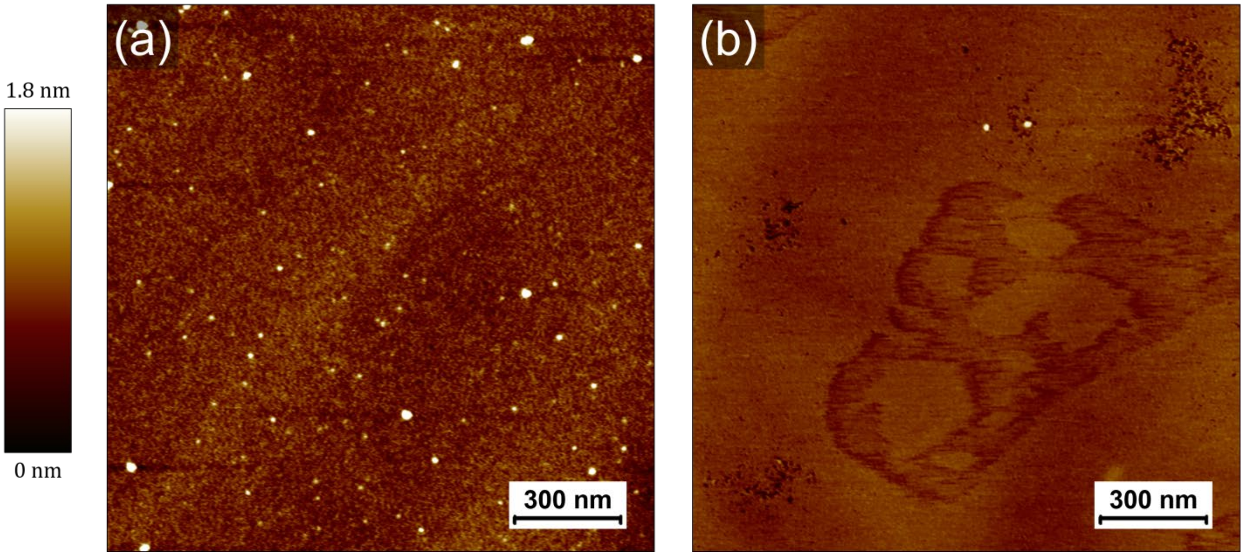

Figure S6. AFM comparison of TBP layers on HOPG (a) before and (b) after 80 min annealing.

Mechanism of ALD growth

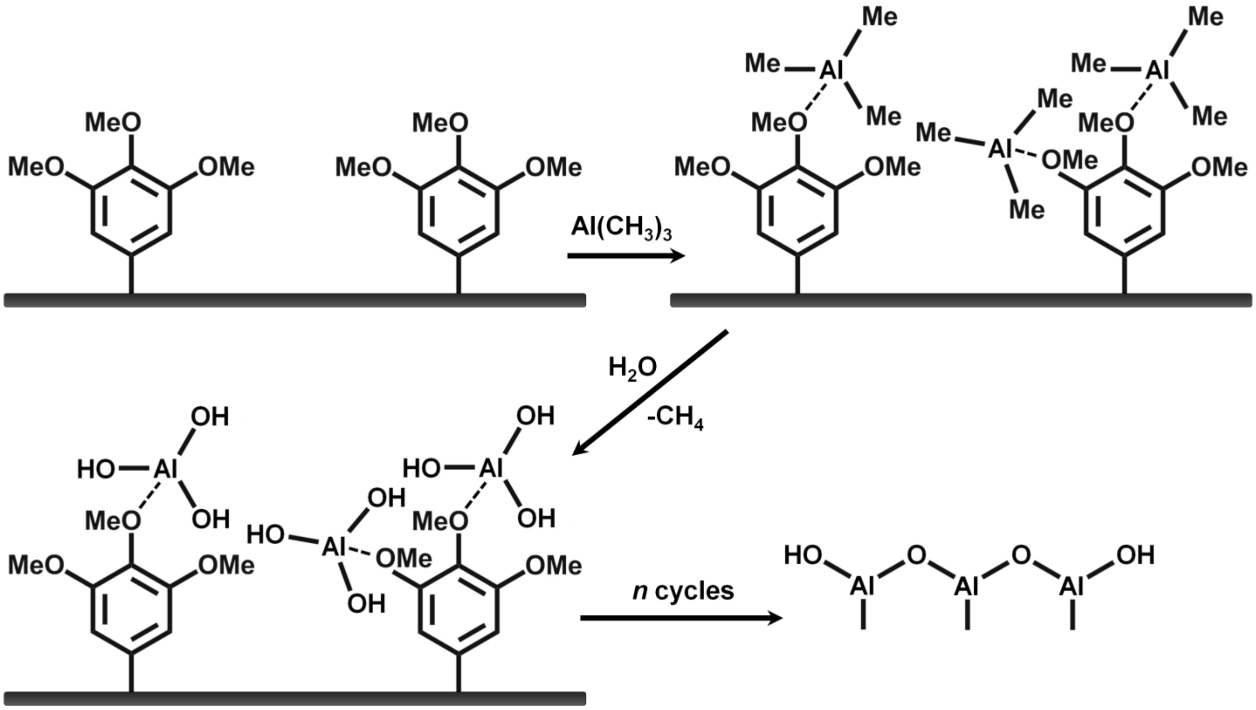

Figure S7. Scheme describing the tentative mechanism of the ALD growth of Al_2O_3. The TMeOP-functionalized sample is initially subjected to a pulse of TMA that binds to the lone pair of electrons in MeO. In presence of water, the methyl groups of TMA are replaced by OH. From this point, classical sequential, self-limiting, ALD process can take place, with TMA reacting on the OH sites.

XPS characterization of the dielectric layer. Al_2O_3 was deposited by ALD on another series of TMeOP-grafted HOPG samples for 10 and 40 cycles to perform XPS measurements. Oxygen contribution comes from both the TMeOP layer and the Al_2O_3. Carbon contribution comes from the HOPG substrate and the TMeOP layer.

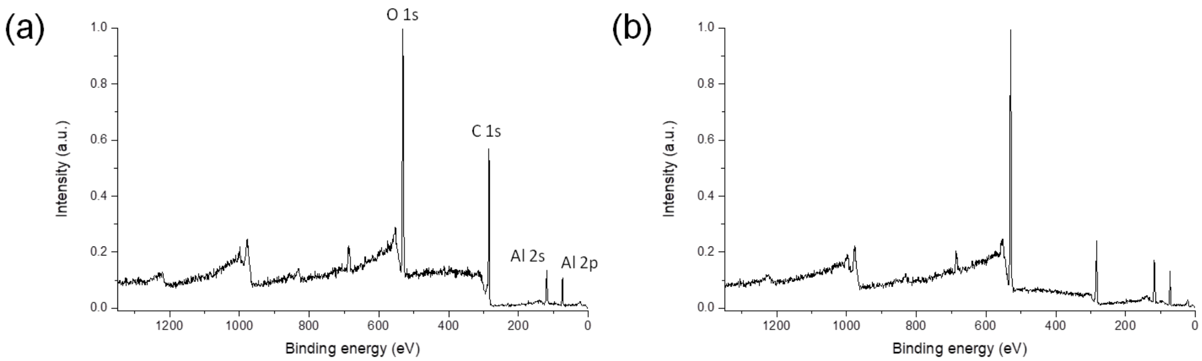

Figure S8. XPS survey spectra of the TMeOP-functionalised sample after (a) 10 cycles and (b) 40 cycles of ALD.

Table S1. Elemental atomic composition of the samples after 10 and 40 cycles. Values are given in percentages.

Samples	O	Al	N	C
10 cycles	36.27	13.82	0.25	49.66
40 cycles	47.88	23.82	0.19	28.11

AFM characterization of the dielectric layer

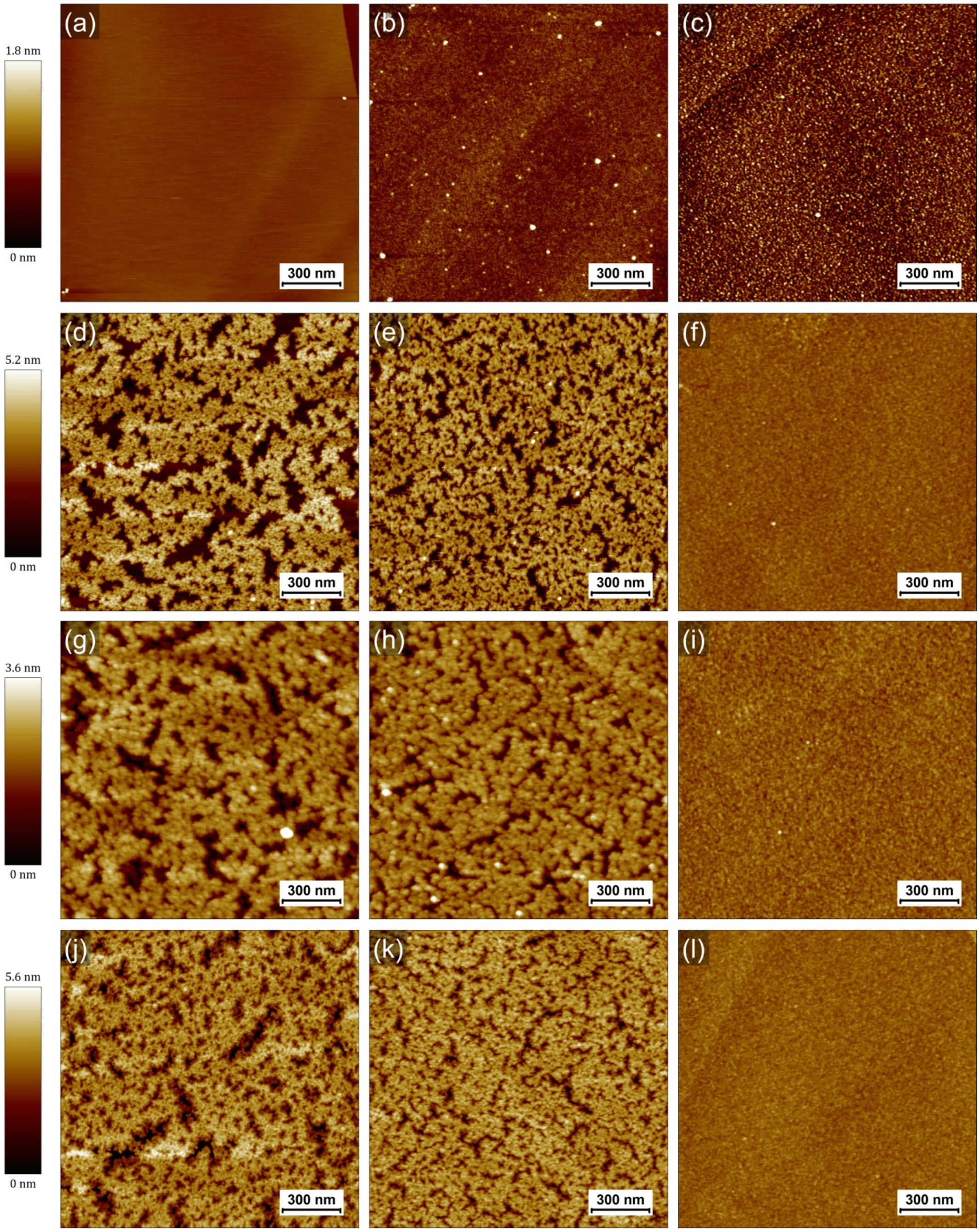

Figure S9. Recap of the AFM images of the three HOPG samples at every step of the ALD growth. Before ALD: (a) HOPG, (b) TBP and (c) TMeOP samples. After 10 cycles: (d) HOPG, (e) TBP and (f) TMeOP samples. After 40 cycles: (g) HOPG, (h) TBP and (i) TMeOP samples. After 80 cycles: (j) HOPG, (k) TBP and (l) TMeOP samples.

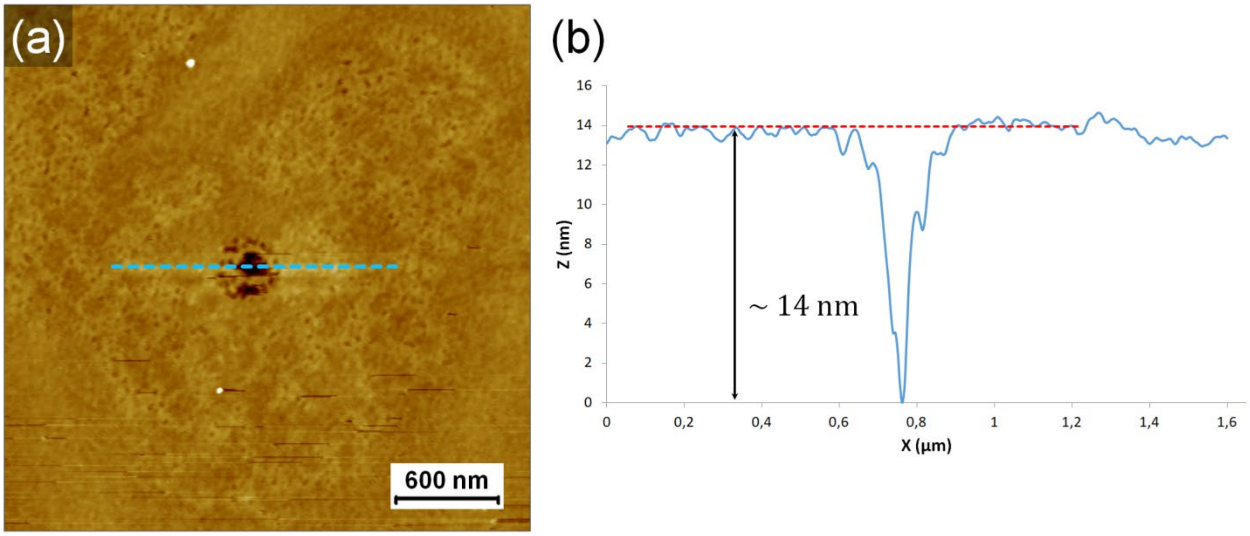

Figure S10. (a) AFM topography image of one of the few holes encountered in the Al_2O_3 layer obtained after 80 cycles of ALD on the TMeOP-functionalized HOPG sample. (b) Line profile along the blue dotted line in (a).

SEM characterization of the dielectric layer

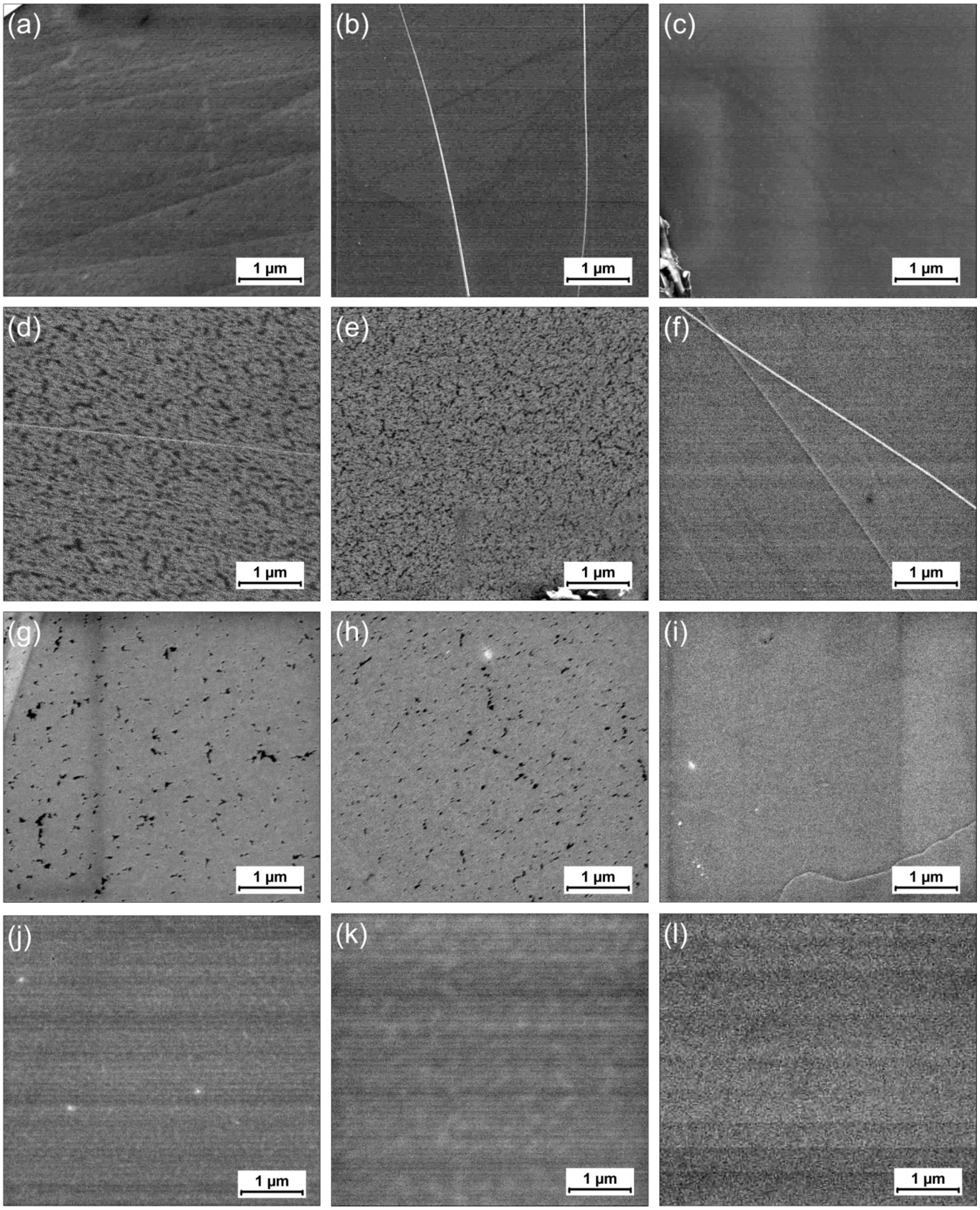

Figure S11. Recap of the SEM images of the three HOPG samples at every step of the ALD growth. Before ALD: (a) HOPG, (b) TBP and (c) TMeOP samples. After 10 cycles: (d) HOPG, (e) TBP and (f) TMeOP samples. After 40 cycles: (g) HOPG, (h) TBP and (i) TMeOP samples. After 80 cycles: (j) HOPG, (k) TBP and (l) TMeOP samples.

Raman characterization after the formation of the dielectric layer. A recap of the Raman spectra of the three HOPG samples recorded (*ex situ*) after every step of the ALD growth (i.e. after 10, 40 and 80 cycles of TMA/H_2O) is presented in figures S12-14.

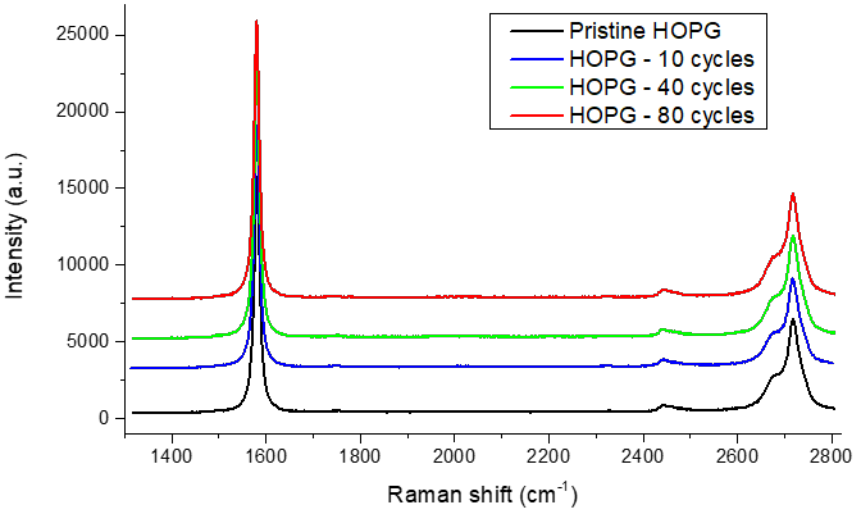

Figure S12. Raman spectra of the bare HOPG sample before ALD and after 10, 40 and 80 ALD cycles.

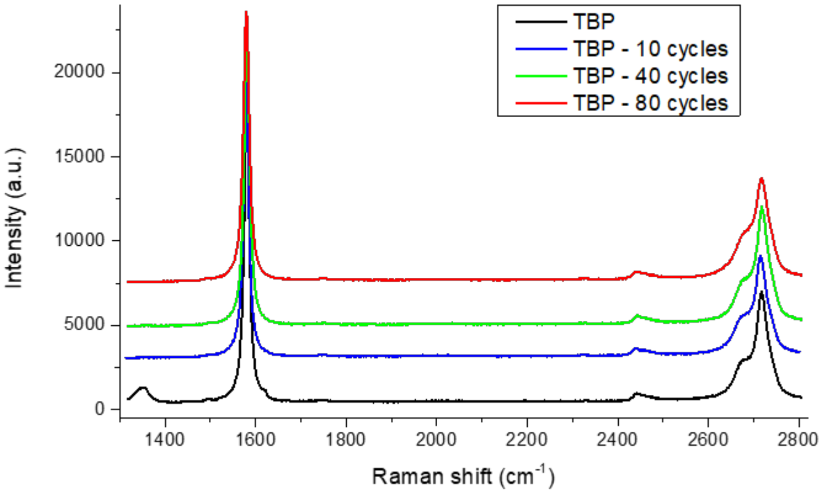

Figure S13. Raman spectra of the TBP-functionalized sample before ALD and after 10, 40 and 80 ALD cycles.

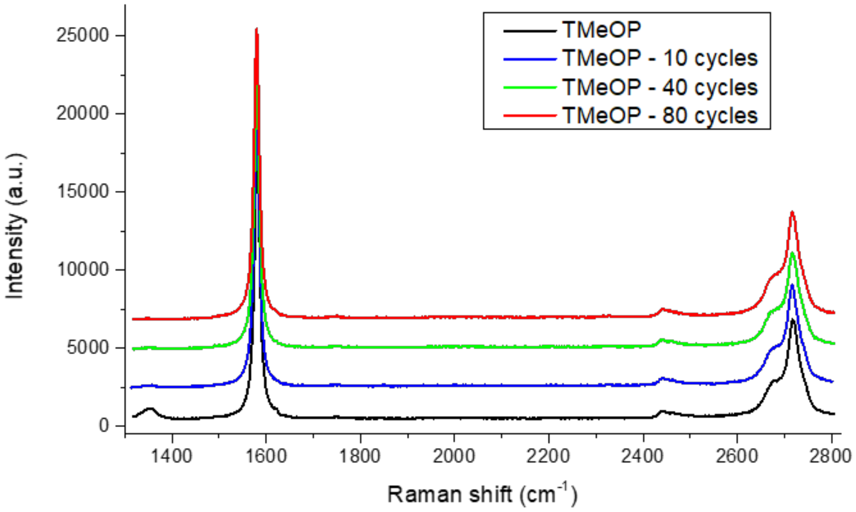

Figure S14. Raman spectra of the TMeOP-functionalized sample before ALD and after 10, 40 and 80 ALD cycles.

AFM and Raman analysis on graphene samples.

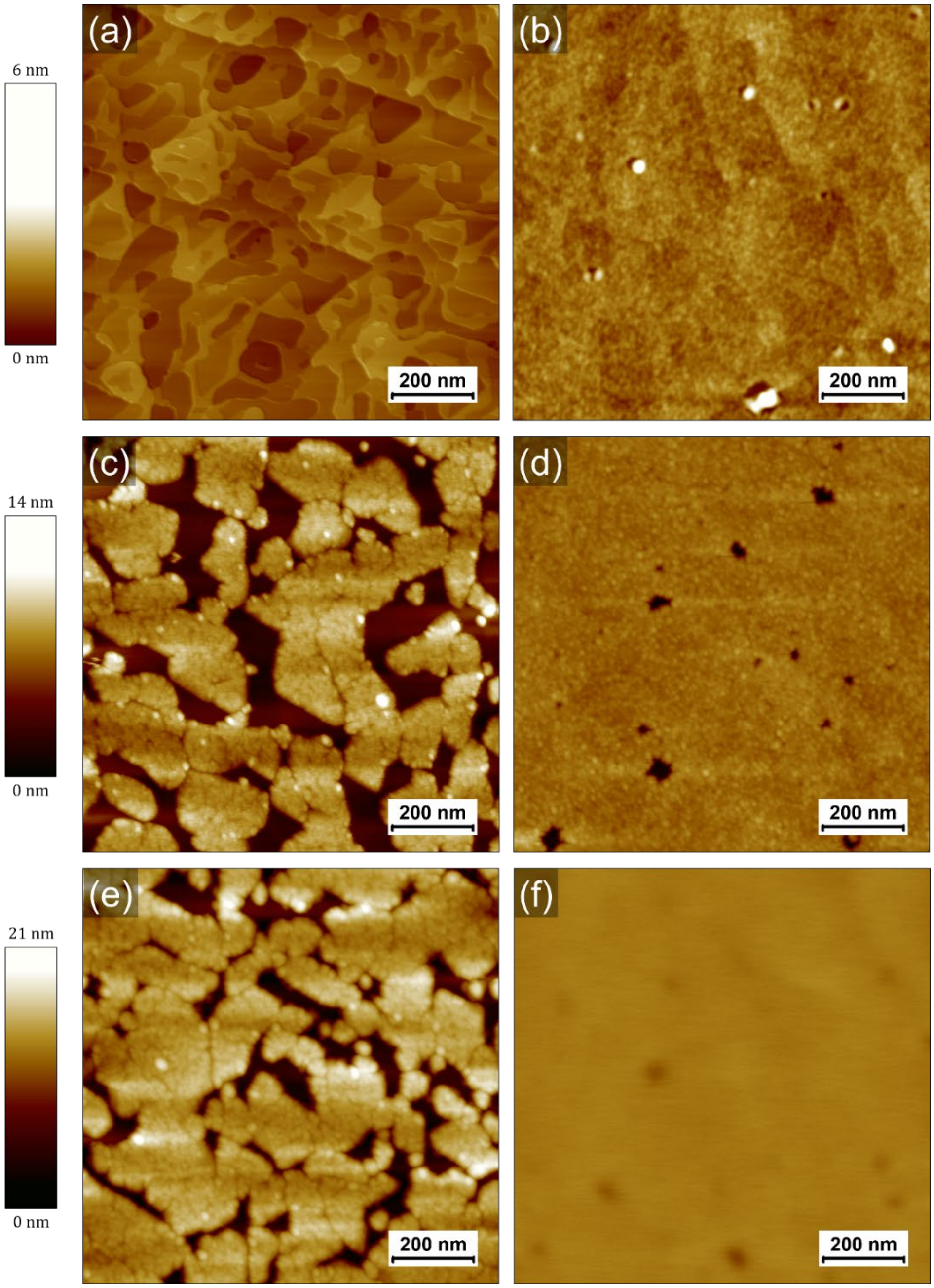

Figure S15. Recap of the AFM images of the two graphene on Cu samples at every step of the ALD growth. Before ALD: (a) bare graphene on Cu and (b) TMeOP-functionalized graphene on Cu. After 40 cycles: (c) graphene and (d) TMeOP samples. After 80 cycles: (e) graphene and (f) TMeOP samples.

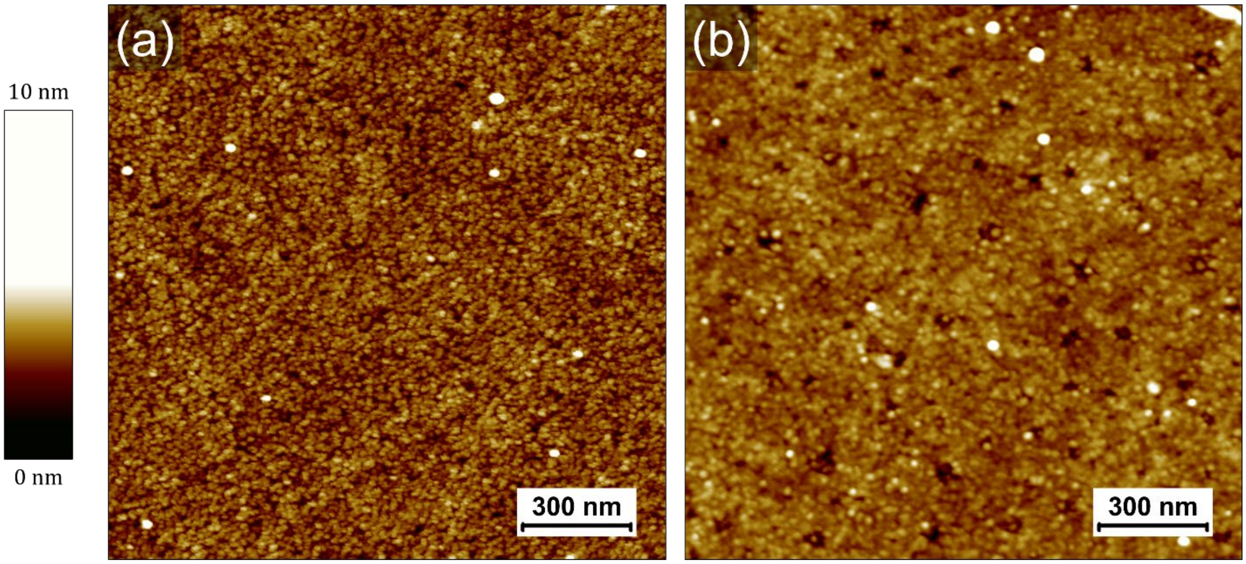

Figure S16. AFM comparison of Al_2O_3 layers obtained after 40 cycles of ALD (a) on bare graphene on SiO_2 and (b) on TMeOP-functionalized graphene on SiO_2.

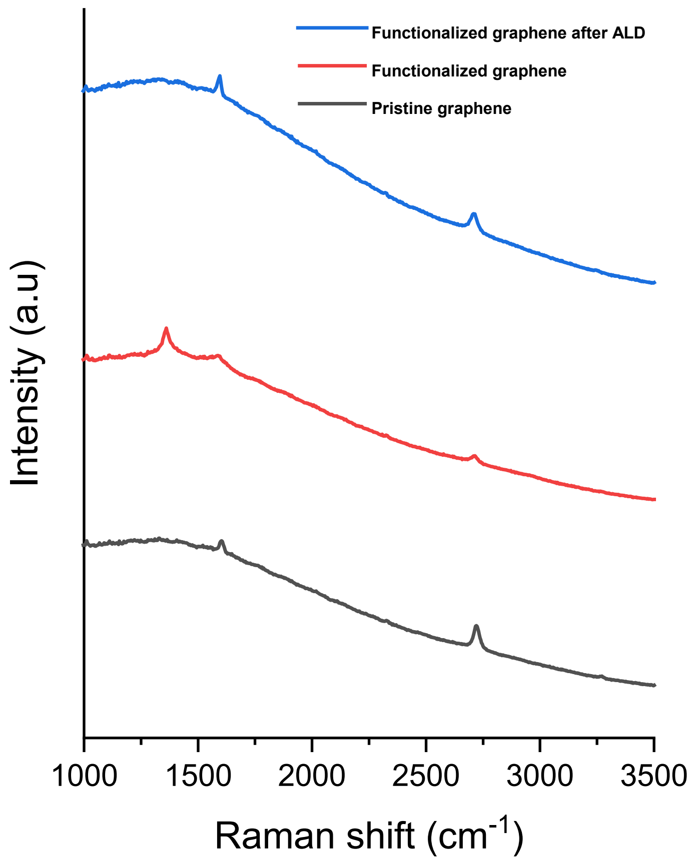

Figure S17. Raman spectra of the pristine graphene on copper (black), TMeOP-functionalized graphene sample before ALD (red) and after 80 ALD cycles (blue).

Electrical measurements. In the device used for the electrical permittivity assessment of the Al_2O_3 film, 60 nm Al_2O_3 was grown (using same conditions as discussed in the main text) on highly doped Si and then a 70 nm Ni electrode was deposited on top with an area of 5.7×10^{-4} cm^2. From this measurement, capacitance and conductance where obtained at different bias (frequency: 500Hz). From that, a conductance of 1.44×10^{-6} S/cm^2 was obtained, and a resistivity of 1.2×10^9 Ω.m. For bulk Al_2O_3 a resistivity of 2.0×10^{11} Ω.m is expected.[1] Compared with bulk Al_2O_3 the film grown on Si is thus 2 orders of magnitude lower, which can be expected given the thin nature of the film.

For the case of the oxide layer grown on the TMeOP layer with a thickness of ~14 nm (including the organic layer) a conductance of 1.1×10^{-5} $S.cm^{-2}$ is obtained. This translates into a resistivity of 6.5×10^8 Ω.m. Therefore, we can see that the resulting film using TMeOP has similar resistivity as that of thicker films (60nm) grown directly on Si.

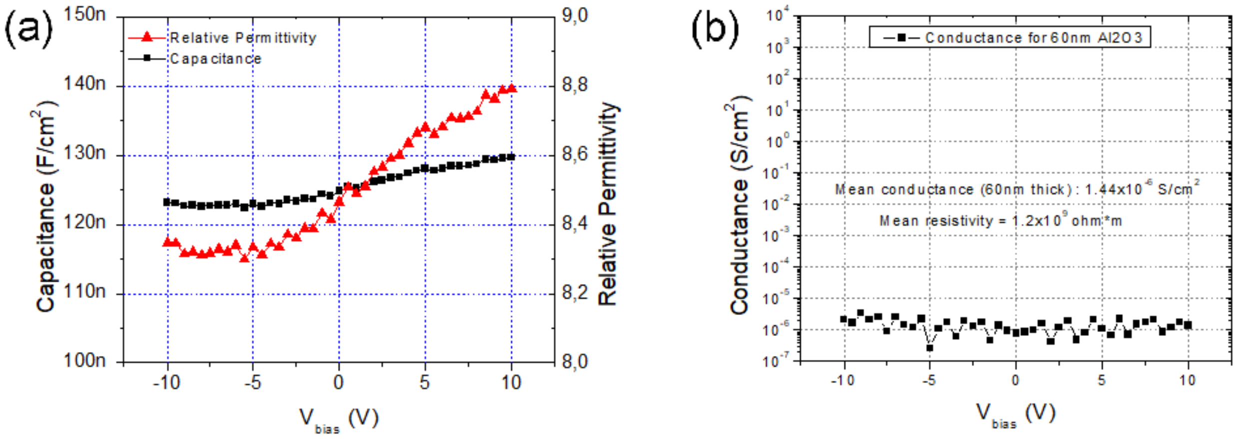

Figure S18. (a) Capacitance and relative permittivity of parallel plate capacitor with 60 nm Al_2O_3 deposited with ALD. The extracted relative permittivity at 0V bias is about 8.5. (b) Conductance of the 60 nm Al_2O_3 film.

Electrical measurements on graphene. Experiment	Conductance	Standard deviation
	S/cm^2	S/cm^2

HOPG + ALD	3.30E+02	3.12E+02
HOPG + TBD + ALD	2.81E+02	2.54E+02
HOPG + TMeOD + ALD	1.11E-05	2.82E-06
GR + TMeOD (40) +ALD	6.25E+03	3.79E+03
GR + TMeOD (80) + ALD	5.55E+03	4.45E+01

Figure S19. Summary of the conductance measurements for the samples analyzed on graphite and graphene substrates.

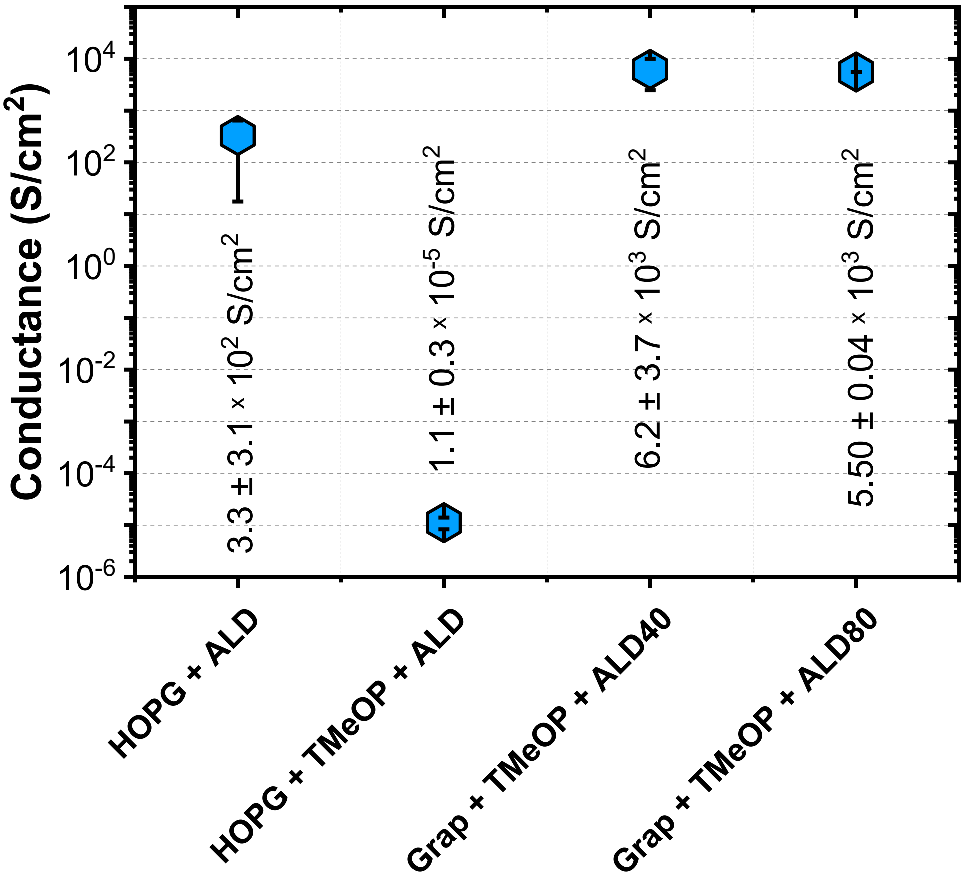

Figure S20. Conductance of the Al_2O_3 films grown on different graphite and graphene substrates.

1. J. F. Shackelford, Y.-H. Han, S. Kim and S.-H. Kwon, *CRC materials science and engineering handbook*, CRC press, 2016.